Presented at the 2006 IEEE 4th World Conference on Photovoltaic Energy Conversion,
May 7-12, 2006, Waikoloa, Hawaii

A SYSTEMATIC APPROACH TO REDUCE PROCESS-INDUCED SHUNTS IN BACK-CONTACTED MC-SI SOLAR CELLS

Filip Granek*, Arthur Weeber, Kees Tool, Ronald Kinderman, Paul de Jong
ECN Solar Energy, P.O. Box 1, NL-1755 ZG Petten, The Netherlands
phone : +31 224 564731, email: p.dejong@ecn.nl

ABSTRACT

One of the main reasons why back-contact (PUM) cells stay somewhat behind in efficiency is because of their lower shunt resistance. A simple method was developed to determine the shunt resistance of the individual process-induced shunt paths. These contributions have led to an electrical model describing the process-induced shunt paths. Individual shunt paths were analysed in detail. Changes in processing were introduced to eliminate the shunting problems. These changes resulted in the shunt resistances beyond 5 kΩcm^2 on 225 cm^2 cells with industrial processing.

INTRODUCTION

New back-contact cell concepts such as the PUM [1] concept are being developed by ECN to lower the €/Wp costs by improving cell and module efficiencies without significantly adding processing costs. A main advantage of PUM cells is that series resistance and shading losses are independent of the cell size. Furthermore, PUM cells have all contacts on the rear side of the cell which allows to manufacture modules with lower series resistance.

Unfortunately a significant percentage of the previously processed PUM cells had relatively poor shunt resistance values [2, 3]. Many cells had shunt resistance values below 2 kΩcm^2, which caused unwanted fill factor and efficiency losses (the fill factor is practically independent of shunt resistance when Rsh > 2 kΩcm^2).

The aim of this work was to determine the reason of poor shunt resistances in the back-contacted mc-Si PUM solar cells, and subsequently to improve the PUM cell processing to increase practical shunt values.

PROCESS-INDUCED SHUNTS IN PUM CELLS

The approach to improve the shunt resistance values in the PUM cells was firstly to identify possible shunt paths. For this purpose a model describing possible shunt paths in the PUM cells was built. This model is schematically shown in Fig. 1. This model applies to all metallization-wrap-through and metallization-wrap-around back-contacted solar cells.

*) F. Granek is now with the Fraunhofer Institute for Solar Energy Systems (ISE), Heidenhofstrasse 2, D-79110 Freiburg, Germany

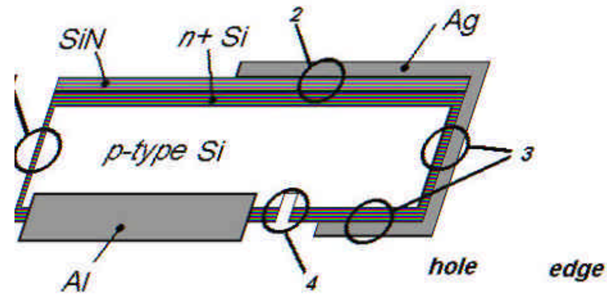

Fig. 1. Schematic representation of the possible process-induced shunt paths in the back-contacted PUM solar cells. See text for comment.

The process-induced shunt paths are then as follows (numbering according to Fig. 1):

1. Poor edge isolation. The emitter at the cell edges is insufficiently disconnected from the base at the rear.
2. Front-side silver paste fired-though the emitter into the base region. Firing-through the emitter can be caused by non-homogeneity of the emitter profile, too high temperature of the contact firing or inadequate silver paste properties (e.g. glass frit aggressiveness).
3. Shunting inside the holes and on the rear side because of silver paste fired-though the emitter into the base region. It is to be expected that the application of the Phosphourous dopant is more difficult inside the holes. This may result in a shallower emitter inside the holes. In addition, the absence of silicon nitride layer makes it easier for the silver paste to penetrate deeper into the silicon than in the case of front side silver paste, where silicon nitride layer is present.
4. Poor emitter isolation around the silver contacts at the back cell side. This isolation step is done at ECN by laser scribing of the rings around the 16 holes on the rear side of the wafer. Non-optimal parameters of laser scribing may result in too shallow ablation of silicon, re-cast of silicon or incomplete emitter removal.
5. Misalignment of the processing steps (not shown in the Fig.1). Four alignment steps are present in the processing sequence of the PUM cells, i.e. screen-printing of the front and rear side silver grid, printing of the rear side aluminium and laser isolation and the rear side. Misalignment of one of this steps will result in a direct shunt.

SEPARATION OF SHUNT PATHS

In order to trace the origin of the poor shunt resistance values in the PUM cells, the shunt resistance of each of the individual shunt paths has to be determined. We have developed a simple method which enables separation of each of the shunt paths.

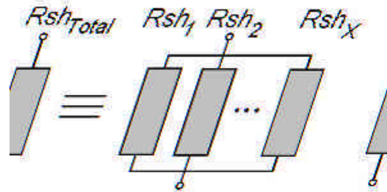

Fig. 2. Total shunt resistance of a PUM can be seen as individual shunt paths connected in parallel.

The shunt paths can be seen as resistors which are connected in parallel (Fig. 2). This parallel resistance can be simply measured in darkness using a digital voltage meter. Disconnection of one of the resistors will result in the increase of the total resistance. By comparing shunt resistance values before (Rsh_A) and after (Rsh_B) each of these disconnection steps, quantification of each of the disconnected shunt path resistance (Rsh_X) is obtained using a basic formula for resistance of parallel connected resistors:

$$\frac{1}{Rsh_A} = \frac{1}{Rsh_B} + \frac{1}{Rsh_X} \qquad (1)$$

Schematic explanation of the principle of the shunt path separation method is shown in Fig. 3. Disconnection of shunt paths is done mechanically in three steps (disconnection steps are numbered according to Fig. 3):

1. Mechanical drilling inside each wrap-through hole removes the silver and emitter inside the hole, which electrically disconnects front and rear side silver metallization (all holes need to be completely drilled away).
2. Milling off the silicon layer over the laser isolation groove on the rear side removes ca. 10 µm of Si, and thereby eliminates laser isolation shunts (all laser isolation grooves need to be milled away).
3. Extra grinding of the edges removes all emitter residuals which eliminates existing edge shunts.

Mechanical drilling can be easily done using a simple drilling device with a small tip. However during drilling some mechanical force need to be applied in order to drill through the hole, so measures need to be taken to avoid breakage of the analysed cell. One should keep in mind that this method is best suited to detect the shunt paths with the lowest shunt value, so it is recommended to process the above mentioned mechanical steps in different orders to obtain most reliable data.

Fig. 3. Simple method to electrically separate shunt paths by mechanically separating base and emitter regions.

The photographs in Fig. 4 show the back side of the PUM cell before (left) and after (right) mechanical drilling steps 1 and 2 of Fig. 3. The enlarged hole shows the removal of the silver metallization and emitter. Also the laser isolation groove was milled off by gently removing approximately 10 µm of silicon, assuring adequate rear side emitter isolation.

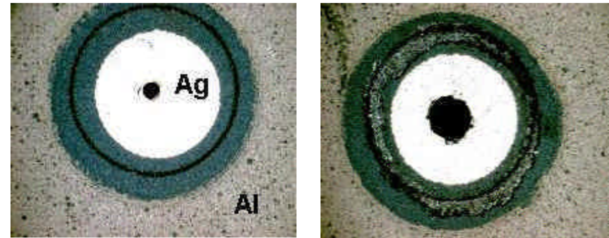

Fig. 4. Rear side silver contact before (left) and after (right) shunt path separation.

Table. 1. Resistance value of the individual shunt paths calculated for the PUM cells processed in 2004 and the cells processed in 2005 after process improvements (average values for 3 and 7 cells processed in 2004 and 2005 respectively).

	Shunt resistance [Ω]	
Shunt path	2004	2005
Laser isolation at the rear side	**6.6**	171.4
Edge isolation	**10.5**	1064.2
Front side silver paste fired-through	57.0	56.9
Rear side silver fired-through	58.0	119.0

Following the described method we have analysed shunted PUM cells that were processed in 2004 and in 2005, respectively. As can be seen in Table 1, PUM cells processed in 2004 suffered from inadequate laser isolation around the emitter contacts at the rear side and from a low quality of the edge isolation. After improvements in

processing, all shunt paths have high resistance values (PUM cells 2005). It is interesting to note that Rsh of rear side silver and front side silver are in the same order of magnitude, although the silver coverage on the rear side is ca. 10 times smaller in comparison to front side silver. This shows the influence of SiN layer on shunting.

ANALYSIS OF THE SHUNT PATHS

Laser isolation on the rear side

In order to isolate rear-side base and emitter contacts 16 rings are laserscribed around each of the wrap-through holes, between silver and aluminium contact areas (see Fig. 5 left). Results in Tab.1 clearly show that the emitter isolation on the rear side was inadequate in case of the PUM cells processed in the year 2004. SEM analysis of the laser grooves revealed that the width and depth of the laser groove was strongly non-uniform (Fig. 4 left). Silicon “bridges” over the laser groove could be observed in the places were the ablation process was non-optimal (Fig. 4 right). These “bridges” are locations where emitter have not been removed, so they form very effective shunt paths.

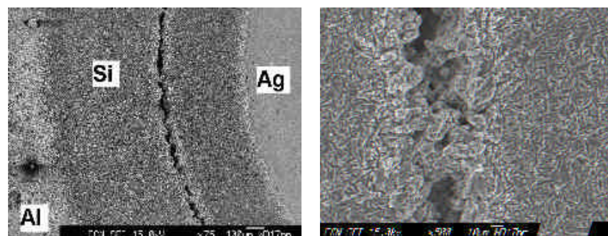

Fig. 5. Microscopic photograph of the laser isolation trench around the emitter contact areas at the cell’s rear side (zoom left x75, right x500).

The parameters of the laser ablation such as the scribing speed, the pulse frequency and the laser current were subsequently optimised. Inhomogenities in the laser trench depth and width have been eliminated. This resulted in an increase of the shunt resistance value of the laser isolation from 6Ω to 170Ω on 225cm² wafer material.

Edge isolation

Edge isolation was performed by grinding the edges with sandpaper. This isolation technique provides, when carried out appropriately, very effective isolation [5]. Minor changes were applied to edge grinding in order to increase the edge isolation quality, which resulted in very high shunt resistance values.

Silver paste firing through the emitter

As mentioned before, silver paste that fires through the emitter causing severe shunting. Silver with the help of glass frit in the silver paste etches into silicon during the high-temperature firing process, penetrating the emitter layer, and can go through the emitter [6]. This way a direct contact to the base can be established, resulting in a shorted junction and poor shunt resistance values.

There are few factors that influence the silver paste firing-through properties. Among them the most important one is the silver paste etch rate of silicon and silicon nitride. If the paste etches too fast into the emitter, then even a very short firing time, which is required to establish low contact resistance, is enough for the silver paste to penetrate the emitter and short the junction. The silver paste etch rate depends on the temperature of the firing process and the properties of the glass frit in the silver paste. Other factors which can influence firing-through the emitter are:

a) presence of the silicon nitride layer. The silver paste must etch through the SiN layer before it can contact the emitter.

b) uniformity of the emitter profile, where shallower junctions increase the chances of shunt.

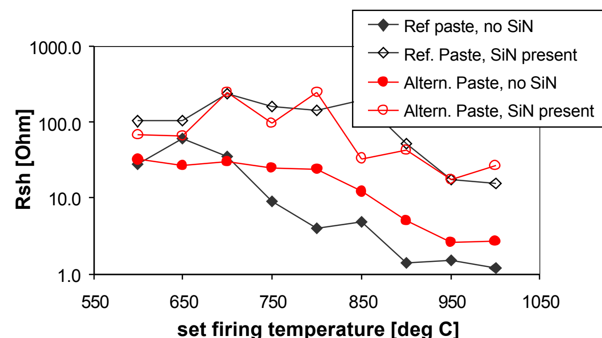

Fig. 8. Shunt resistance of the cells fired in the wide temperature range.

In order to quantify the influence of the above mentioned parameters on the shunt resistance values, a firing experiment was carried out. Onto 12.5x12.5 cm^2 mc-Si samples with the standard cell concept using screen-printed front-side silver paste and rear full area aluminium paste were fired over a wide temperature range. We have tested two silver pastes, i.e., a reference paste (Ref.) which is used for the PUM cell processing and an experimental paste as an alternative (Altern.) with lower Si etch rate. Samples with and without SiN layer on the front side were processed. Although all samples have the same thickness and size, it is to be expected that during firing the presence or absence of the SiN layer causes the actual temperature of these samples to be different. The shunt resistance results are shown in Fig. 8. It can be seen that in the relevant set firing temperature range (800-1000 °C) Rsh of the cells fired with SiN layer is approximately 10 times higher than in the case where silver paste was screen-printed directly on the emitter surface, proving that SiN layer very strongly reduces shunting risk. Shunt resistance of the cells with alternative paste on the samples without SiN exhibit ca. 2-3 higher Rsh values in comparison to the reference paste.

IMPROVED PROCESSING OF THE PUM CELLS

In order to improve PUM cells processing, the lessons learned from the shunt paths analysis were used to introduce process changes that are industrially applicable. Laser isolation of the emitter contact at the rear side was optimised. Edge isolation was improved. In order to decrease firing-through the emitter of the silver paste the emitter on the rear side was diffused deeper than the front-side emitter and the silver paste on the rear is chosen different from the front-side silver paste. Moreover the amount of silver contacting the rear-side emitter was reduced.

These changes resulted significant increase shunt resistances with values beyond 5 kΩcm^2 on 225 cm^2 cells with industrial processing and top efficiency of 16.7 % [4].

CONCLUSIONS

The individual shunt contributions were identified by electrical separation of the process-induced shunt paths. The individual shunt values provide direct feedback on the settings and parameters of a single process step.

All the findings of the shunt related investigations were used to improve processing of the PUM cells. Average shunt resistance of the cells processed in 2005 [4] equals 5.2 kΩcm^2 on 150mm cells, which is a major improvement when compared to cells produced in 2004 [3]. The feedback of the shunt analysis into processing improvements led to a top cell efficiency of 16.7% absolute on average material quality. This is an improvement of 0.5% absolute when conventional H-pattern cells were processed on the same material.

ACKNOWLEDGMENTS

We gratefully acknowledge the financial support from the Dutch Economy, Ecology and Technology (E.E.T.) program. E.E.T. is an initiative of the Ministry of Economic Affairs, the Ministry of Education, Culture and Science and the Ministry of Public Housing, Physical Planning and Environment.

REFERENCES

[1] J.H. Bultman et al., “Interconnection through vias for improved efficiency and easy module manufacturing of crystalline silicon solar cells”, *Solar Energy Materials & Solar Cells*, **65** (2001), pp.339-345.

[2] J.H. Bultman et al., “Fast and easy single step module assembly for back-contacted c-Si solar cells with conductive adhesives” , 3rd WCPVSEC, Osaka, 2003.

[3] P.C. de Jong et al., “ Single-step laminated full-size PV modules made with back-contacted MC-Si cells and conductive adhesives”, 19th EPVSEC, Paris, 2004.

[4] A. Weeber et al., “How to achieve 17% cell efficiencies on large back-contacted mc-Si solar cells”, submitted to this conference.

[5] A. Hauser et al., “Comparison of different techniques for edge isolation”, 17th EPVSEC, Munich, 2001.

[6] G. Schubert et al., “Current transport mechanism in printed Ag thick film contacts to an n-type emitter of a crystalline silicon solar cell”, 19th EPVSEC, Paris, 2004.